Performance analysis of ice storage tank with smooth-tube and corrugated-tube heat exchangers based on numerical simulation

Yaran Wang [a], Juan Hou [a], Pengkun Zhou [a], Zhihao He [a], Shen Wei[b], Shijun You [a], Huan Zhang [a] , Xuejing Zheng [a,*]

[a] School of Environmental Science and Engineering, Tianjin University, Tianjin 300350, PR China

[b] The Bartlett School of Construction and Project Management, University College London (UCL), 1-19 Torrington Place, London WC1E 7HB, United Kingdom

[*] Corresponding author, Email: zhengxuejing@tju.edu.cn

Abstract

The ice storage system is of great value to improve the flexibility of building cooling load. In this paper, the two-dimensional physical models of smooth-tube and corrugated-tube heat exchangers ice-storage tank is established with consideration of natural convection. The ice storage process of tubes is numerically simulated using Computational Fluid Dynamics (CFD). The effects of structural parameters on the ice storage performance are comprehensively analyzed, including the pitch and height of corrugation. The results indicate that the ice storage duration of the corrugated-tube heat exchanger is shortened by 7.1% compared with that of the traditional smooth-tube heat exchanger, which is due to the fact that corrugations disrupt the development of the boundary layer and strengthen the fluid mixing. There is the thicker ice layer outside

the corrugated tube in comparison with the smooth tube at the same time. In addition, the influence of the corrugated tube structure on its ice storage performance is studied by varying the corrugation pitch and height. If the corrugation pitch is decreased by 41.7% and the corrugation height is increased by 28%, the heat transfer performance of corrugated tubes is improved by 10.3% and 29.4%, respectively.

Keywords: Ice storage; Corrugated tube; Cold thermal energy storage (CTES); Performance analysis

Nomenclature

		λ	Thermal conductivity (W/(m·K))
		ρ	Density (kg/m^3)
u	Velocity along x-axis (m/s)	μ	Dynamic viscosity (kg/(m·s))
v	Velocity along y-axis (m/s)	Γ	Latent heat (J/kg)
T	Temperature (°C)	τ	Time (s)
p	Pressure (Pa)		
c	Specific heat capacity (J/(kg·°C))	subscripts	
g	Gravity (m/s^2)	s	Solid
H	Enthalpy (J/kg)	l	Liquid
S	Source (W/m^2)	S	Sensible
		L	Latent
Greek letters		p	PCM
β	Liquid fraction	h	Heat

1. Introduction

As society develops and humanity progresses, energy demand is increasing. The consumption of primary energy is expected to increase globally by 48% by 2040 [1]. Thermal energy storage (TES) not only reduces the mismatch between supply and demand but also improves the performance and reliability of energy systems, which means it plays an important role in energy conservation [2]. Compared with other energy storage systems, the latent heat thermal energy storage (LHTES) system has the advantages of large heat storage capacity and stable operating temperature [3]. In cold storage systems, water is the most commonly used phase change material (PCM) in installations among other reasons because of the high latent heat capacity, availability and low cost [4]. Ice/water system has been analyzed in different configuration such as with encapsulation [5], ice slurries [6] and internal/external melt-ice-on-coil systems [7-9]. The internal melt-ice-on-coil tank is widely used for ice storage [10]. Its ice storage tube is placed in the ice storage tank. The low-temperature glycol solution flows within the tube, and the water freezes outside the tube.

However, thermal resistance between the refrigerating medium and water increases with the thickness of ice due to the low heat transfer coefficient of ice [11]. The coil heat transfer structure has many advantages and superior performance, which has been widely used in many areas to enhance heat transfer [12]. At present, the research on coil heat exchanger is mainly focused on two aspects: numerical simulation and experimental study [13]. Ghorbani et al. [14] investigated the mixed convection heat

transfer in helical coiled tube heat exchanger experimentally. They found that the heat transfer coefficient decreased as the surface area increased. The heat transfer coefficient enhances with increasing the dimensionless tube pitch. Afsharpanah et al. [15] studied the effects of dimensionless parameters on the charging rate of a shell and dual coil ice storage unit equipped with connecting plates as heat transfer enhancers. The results suggested that the geometrical optimization of the proposed ice storage with the helical pitch length/storage height ratio, helical coil distance/storage diameter ratio, and helical coil diameter/storage diameter ratio parameters can improve the charging process up to 16.69%, 7.25%, and 18.84%, respectively. Yang et al. [16] investigated the ice storage process of the ice-on-coil storage plate with different refrigerant inlet temperatures. The results showed that a lower refrigerant inlet temperature contributed to the higher heat exchange efficiency, cold storage rate and cold storage capacity. Bi et al. [9] exploited a new ice-storage system with a closed (CIST) and an open (OIST) ice-storage tank and studied the external ice melting process experimentally. The experiment indicated that the cold release rate of CIST is more stable than that of OIST under the same conditions. Also, the cold release rate increases with the increasing volumetric-flow rate. Afsharpanah et al. [17] evaluated the impacts of various dimensionless parameters in a small-scaled ice container with two rows of serpentine tubes and connecting plates as extended surfaces on the charging process in the container. The results showed that higher tube pitch length/container height ratio, tube row distance/container width ratio, plate area/the maximum plate area ratio and plate thickness/tube diameter ratio, and lower tube diameter/container diagonal length ratio values lead to enhanced charging

rates. In addition, the inclusion of nanomaterials for obtaining a better thermal conductivity of fluids was the subject of many studies [18]. Afsharpanah et al. [19] examined the freezing process of four different nano-enhanced phase change material (PCM)-porous composites. The evaluations indicated that by using copper foam with a porosity of 0.95 and CuO nanomaterials with a concentration of 0.03 at the same time, the phase change rate can be elevated by 92.5%. Zaboli et al. [20] evaluated turbulence heat transfer and nanofluid flow in a shell and corrugated coil tube heat exchanger numerically. The results indicated that at high Reynolds number, utilizing a five-lobe cross-section causes augmentation in Nusselt number and pressure drop by about 4.8% and 3.7%, respectively. Afsharpanah et al. [21] also investigated the compound heat transfer enhancement of a cylindrical-shaped unit equipped with double helically coiled coolant tubes using connecting plates and nano additives as heat transfer augmentation methods. The results suggest that using nano additives and the connecting plates together is a promising way to enhance the solidification rate by up to 29.9%. Laouer et al. [22] examined the combined effect of a uniform magnetic field and nanoparticle volume fraction on the melting process of copper-water (ice) as nano-enhanced phase change material (NePCM). The results showed that the melting time is considerably extended at high Rayleigh number as the Hartmann number is increased and addition of nanoparticles notably contributes to the shortening of melting time at low Rayleigh number.

In recent years, more and more research has been conducted on the optimization design of coil heat transfer structure, such as inserting fins [23],using corrugated coil

[24] and so on. Jannesari et al. [25] compared the performances of two heat transfer enhancement methods including usage of thin rings and annular fins around coils. They found that diagonal thin rings had better performance with respect to annular fins. Agyenim et al. [26] studied the enhancement performances of circular and longitudinal fins. Longitudinal fins proved to be better than circular fins. Ismail et al. [27] investigated the enhancement of heat transfer in PCM with a radial finned tube. It was found that the increment in the fin diameter accelerated the velocity at the interface and reduced the solidification time. Afsharpanah et al. [28] proposed an innovative anchor-type longitudinal fin design to cope with the sluggish phase change process in shell-and-tube ice storage units. The simulations showed that the melting process is much slower than the solidification process, and the presence of fins can be more influential on the melting process. In addition, corrugated tube can be used to enhance heat transfer performance. Yang et al. [29] studied the turbulent friction and heat characteristics of spirally corrugated tubes with various geometrical parameters. They concluded that spirally corrugated tubes had better thermal performance than smooth tubes. Olfian st al. [30] evaluated numerically the thermal performance of evacuated tube solar collectors integrated with phase change material in the corrugated U-shaped tube. The results showed that the corrugated tube increases the collector efficiency by 21.55% compared to smooth tube and four-lobe corrugated tube retains the collector' s operation temperature up to 40 ℃. Zaboli et al. [31] evaluated heat transfer and fluid flow in a corrugate coil tube with different lobe-shaped cross-sections numerically. The results showed that five-lobe cross-section rises the Nusselt number and pressure drop

by 9.1% and 3.7%, respectively. Li et al. [32] investigated the turbulence heat transfer enhancement mechanism of transverse corrugated tubes (TCTs) with different corrugation heights. They found that the heat transfer characteristics were related to the relative magnitudes of the corrugation height and the viscous sublayer thickness and obtained best heat transfer enhancement with a roughness height of about three times the viscous sublayer thickness. Moghadam et al. [33] investigated the heat transfer and pressure drop in a corrugated tube with coil wire numerically. Results indicate that the geometrical and fluid flow parameters have significant effects on the thermal performance of the system. Computational fluid dynamics (CFD) has been also widely used to investigate the flow and heat transfer characteristics of corrugated tubes [24]. Agra et al. [34] compared the heat transfer and pressure drop performances of two helically finned tubes and two corrugated tubes using CFD. They founded that the heat transfer coefficient of corrugated tubes is lower than that of helically tubes. Haervig et al. [35] studied the fully-developed heat transfer enhancing flow field in sinusoidally and spirally corrugated tubes using CFD. It found that the performances of the corrugated tubes were reduced at higher corrugation heights. Mohammed et al. [36] studied the thermal characteristics of transverse corrugated tubes with different geometrical parameters and *Re* values by CFD. The results showed that with water as the PCM, the highest *Nu* was obtained with relative roughness height e/d = 0.1. Afsharpanah et al. [37] investigated the enhancement obtained by installing several networks of horizontal and vertical plate fins on the serpentine HTF tubes and tested several nanomaterial-based solutions as alternatives to the pure PCM. The results

showed that the combination of plate-fin network and MWCNT particles is a promising technique that can expedite the ice formation rate by up to 70.14%.

In previous studies, most of the inner corrugated tubes, such as the transversely corrugated tube and the helically corrugated tube have been studied, while few research focused on the enhancement of the heat transfer performances of the outward corrugated tube. In this paper, the heat transfer performance and the influence of the corrugated structure of a symmetric corrugated tube heat exchanger on its ice storage performance are investigated by the numerical simulation. The enhancement performance of the corrugated-tube heat exchanger during the ice storage process is analyzed by comparing the temperature distribution characteristics of the two heat exchangers. More importantly, there is currently few research on the structural parameters of symmetrical outward corrugated tubes, while the influence of corrugation pitch and height on the ice storage process is crucial for the practical application of corrugated tubes in engineering. Therefore, the influence of the corrugated tube structure on its ice storage performance is studied by varying the corrugation pitch and height. The numerical simulation results provide the reference for the application of corrugated tube in practical engineering.

2. Method

2.1 Numerical method

Due to the limitations of experimental equipment and conditions, the physical phenomena inside the ice storage tank cannot be well observed. In order to investigate

the effects of corrugation geometry on ice storage performance, an unsteady model of the ice storage process is established, numerically solved using the commercial CFD software ANSYS Fluent, which is validated by the experiment results of the smooth-tube and corrugated-tube heat exchangers.

2.1.1 Physical model

This paper studies the cooling storage model of external ice melt, taking the ice-storage tank as the research object. The schematic structural diagrams of the two heat exchangers are shown in Fig. 1 and Fig. 2.

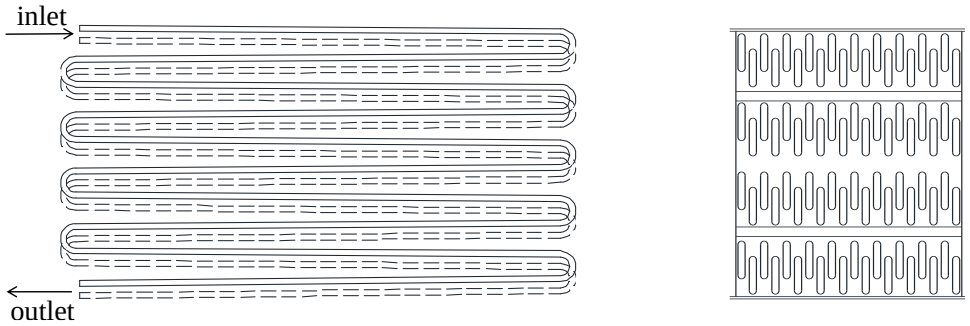

(a) Front view (b) Side view

Fig. 1. Structural diagram of smooth-tube heat exchanger

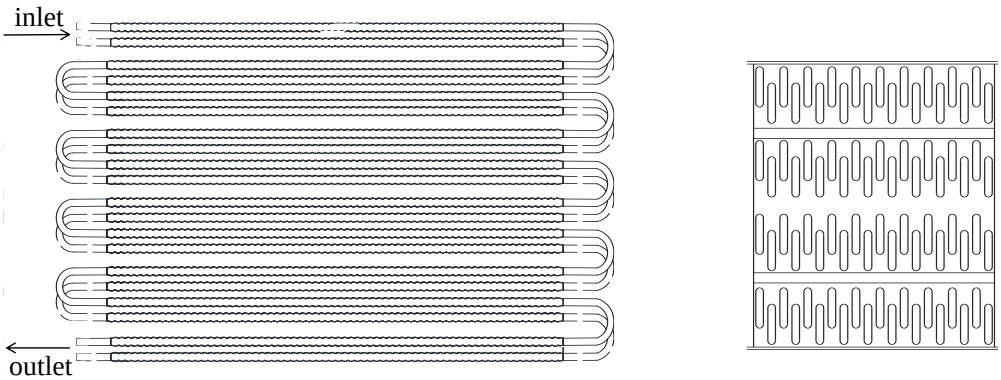

(a) Front view (b) Side view

Fig. 2. Structural diagram of corrugated-tube heat exchanger

The overall structural model of the ice storage tank tubes is complicated, so the ice-water phase change heat transfer model of the complete tube is simplified and a two-dimensional model is established for the study. The tubes in the ice storage tank are parallel, which can be regarded as a symmetrical arrangement of 20-way straight tubes. As shown in Fig. 3 and Fig. 4, the tubes with axial section and radial section can be regarded as evenly arranged in the ice-storage tank. The length of the straight section of tubes is 1590mm, and the diameter of smooth tube is 20mm. The corrugation height of the corrugated-tube heat exchanger is 25mm, and the valley height is 20mm. During the simulation process, the low-temperature ethylene glycol solution inside the tubes is regarded as internal heat source to provide energy for the solidification of water outside the tubes.

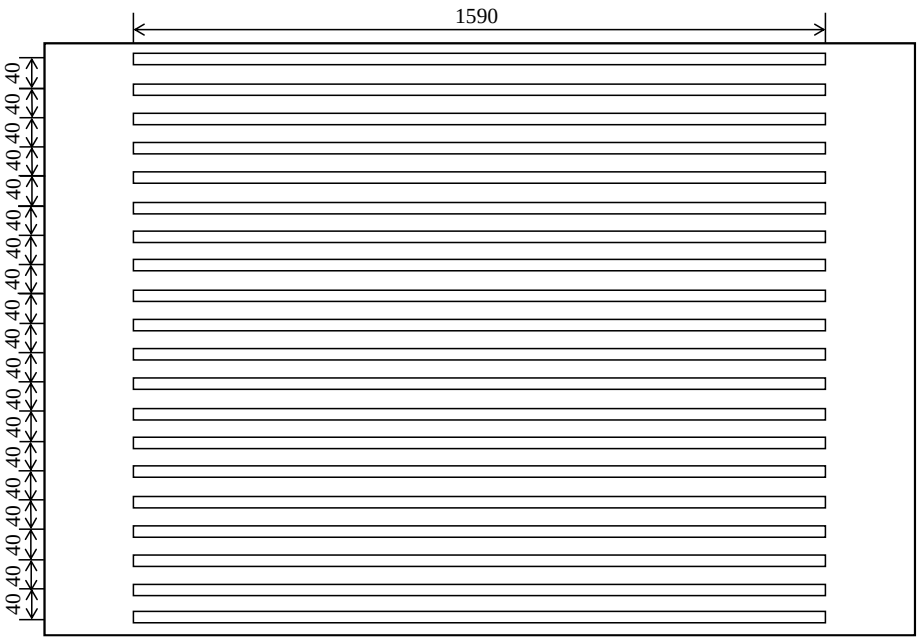

(a) smooth-tube heat exchanger

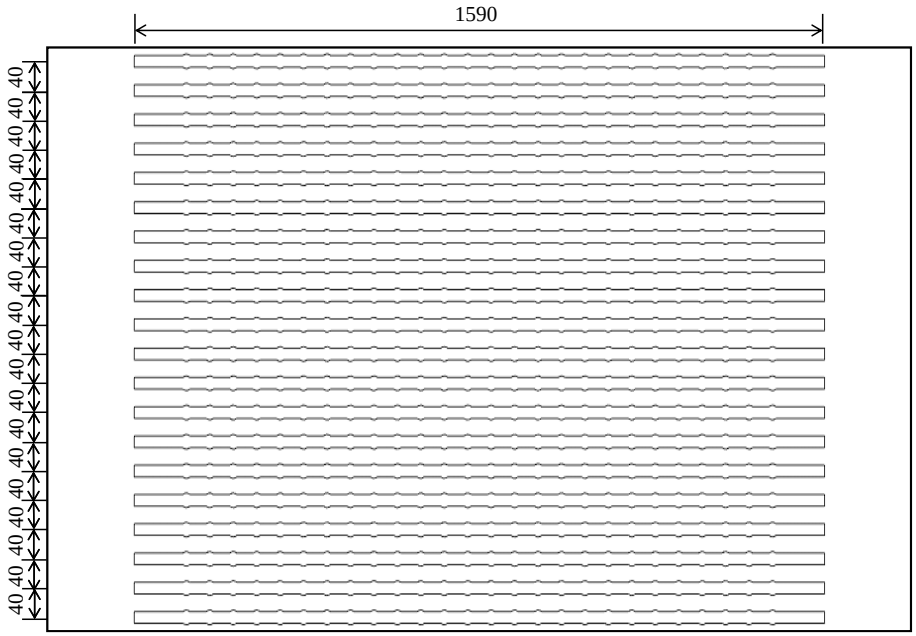

(b) corrugated-tube heat exchanger

Fig. 3 Physical model of axial section

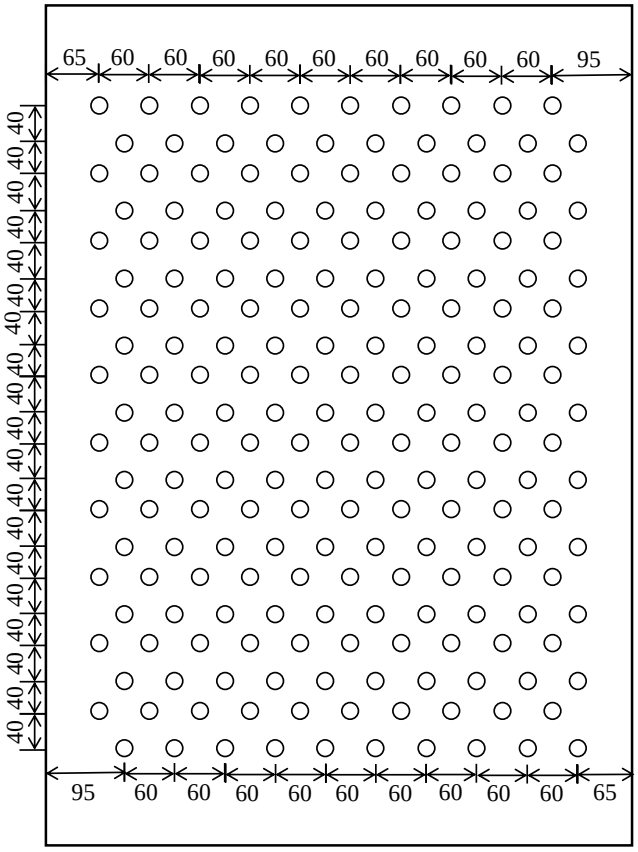

Fig. 4 Physical model of radial section

The purpose of the two-dimensional model of the smooth-tube and corrugated-tube heat exchangers is to be able to fast and accurately simulate the temperature distribution characteristics for subsequent research and analysis. The model of the ice storage system is simplified by considering the following assumptions:

(1) The walls of ice-storage tank are adiabatic with no cold loss;

(2) The impact of the thickness of the tubes wall on the heat transfer is ignored;

(3) The flow inside the ice storage tank is assumed to be laminar;

(4) The temperature of the PCM (water) in the ice-storage tank is well-distributed and constant at the initial time;

(5) Water is isotropic in both liquid and solid phase states, and the physical parameters of water are constant, except for the density;

(6) All interfaces are not deformed, and the liquid-solid interface is slip free.

2.1.2 Mathematical model

The method used for modelling the solidification/melting process in the commercial CFD software of ANSYS Fluent is the enthalpy-porosity technique [38], which simplifies the calculation by taking temperature and enthalpy together as unknown variables to obtain the energy equation containing the two variables, and then to obtain the temperature distribution by the relationship between the temperature and the enthalpy.

Instead of tracing the two-phase interface explicitly, the liquid fraction β is

introduced to describe the solid-liquid distribution:

$$\beta = \begin{cases} 0 & , \quad \mathrm{H} \le H_{\mathrm{s}} \\ \dfrac{H - H_{\mathrm{s}}}{H_{\mathrm{l}} - H_{\mathrm{s}}} & , \quad H_{\mathrm{s}} < H < H_{\mathrm{l}} \\ 1 & , \quad H \ge H_{\mathrm{l}} \end{cases} \tag{1}$$

where H_{s} (℃) and H_{l} (℃) are the enthalpy of solid phase and liquid phase at 0 ℃, respectively. If the enthalpy of ice at 0 ℃ is 0 J/kg, the enthalpy of water at 0 ℃ is 333146 J/kg.

The mass conservation equation is expressed as [11]:

$$\frac{\partial \rho}{\partial \tau} + \frac{\partial (\rho u)}{\partial x} + \frac{\partial (\rho v)}{\partial y} = 0 \tag{2}$$

where ρ (kg/m^3) is the density of the PCM, u (m/s) is the velocity component along the x-axis and v (m/s) is the velocity component along the y-axis.

The momentum equations are expressed as [39]:

$$\frac{\partial (\rho u)}{\partial \tau} + u\frac{\partial (\rho u)}{\partial x} + v\frac{\partial (\rho u)}{\partial y} = \frac{\partial}{\partial x}\left(\mu \frac{\partial u}{\partial x}\right) + \frac{\partial}{\partial y}\left(\mu \frac{\partial u}{\partial y}\right) - \frac{\partial p}{\partial x} \tag{3}$$

$$\frac{\partial (\rho v)}{\partial \tau} + u\frac{\partial (\rho v)}{\partial x} + v\frac{\partial (\rho v)}{\partial y} = \frac{\partial}{\partial x}\left(\mu \frac{\partial v}{\partial x}\right) + \frac{\partial}{\partial y}\left(\mu \frac{\partial v}{\partial y}\right) - \frac{\partial p}{\partial y} - g \tag{4}$$

where μ (kg/(m·s)) is the dynamic viscosity of PCM, τ (s) is the time, p (Pa) is the pressure and g (m/s^2) is the gravity acceleration.

The energy equation is [40]:

$$\frac{\partial (\rho H)}{\partial \tau} = \frac{\partial}{\partial x}\left(\lambda \frac{\partial T}{\partial x}\right) + \frac{\partial}{\partial y}\left(\lambda \frac{\partial T}{\partial y}\right) + S_h \tag{5}$$

where T (℃) is the temperature of PCM, λ [W/(m·℃)] is the thermal conductivity of water, S_{h} (W/m^2) is the source term.

As for PCM, the total enthalpy consists of the sensible enthalpy H_{S} and the latent

heat H_{L} [41]:

$$H = H_{\mathrm{S}} + H_{\mathrm{L}} \tag{6}$$

$$H_{\mathrm{S}} = \begin{cases} H_{\mathrm{l}} + \int_0^{\mathrm{T}} \mathrm{c_{pl}} dT & \mathrm{T} > 0 \\ H_{\mathrm{s}} - \int_{\mathrm{T}}^0 \mathrm{c_{ps}} dT & \mathrm{T} < 0 \end{cases} \tag{7}$$

$$H_{\mathrm{L}} = \beta \cdot \Gamma \tag{8}$$

where H (J/kg) is the enthalpy of PCM, c_{p} [J/(kg·℃)] is the specific heat capacity of PCM, Γ =333146 J/kg presents the latent heat of PCM.

During the ice storage process, the density of water outside the tube changes with the decreasing temperature, resulting in the natural convection. While the density of water is the largest at 4 ℃, which does not conform to the Boussinesq hypothesis. In order to reflect the actual situation of natural convection during the ice storage process, the variation of fluid density with temperature in the buoyancy term of the momentum equation is adopted as follows [42]:

$$\rho = \sum_{n=0}^{5} C_n T^n \tag{9}$$

where $C_0 = 9.998396 \times 10^{-1}$, $C_1 = 6.798490409 \times 10^{-5}$, $C_2 = -9.106280624 \times 10^{-5}$, $C_3 = 1.005301157 \times 10^{-7}$, $C_4 = -1.126745085 \times 10^{-9}$, $C_5 = 6.591980242 \times 10^{-12}$

The thermal conductivity of PCM varies with temperature as:

$$\lambda = 2.22 \cdot (1 - \beta) + 0.55 \cdot \beta \tag{10}$$

There is no cold loss between the ice-storage tank and the surroundings:

$$\frac{\partial T}{\partial x} = \frac{\partial T}{\partial y} = 0 \tag{11}$$

The fluid temperature in the ice-storage tank is well-distributed at the initial

moment, and the initial state of PCM is liquid. The initial conditions are shown as follows:

$$\tau = 0: \quad T = 10℃, \quad \beta = 1 \tag{12}$$

2.1.3 Numerical solution

In this study, the two-dimensional numerical simulation of the ice-storage tank is calculated using the ANSYS Fluent. The water in the tank is closed without flow, so the laminar model is used for simulation research. The initial temperature of water is set to 10 ℃. The governing equations are solved in the pressure-based solver, which is the only option for solidification/melting model in Fluent [41]. To process the pressure-velocity coupling, the SIMPLE algorithm is applied due to the short convergence item. The least-squares cell-based method is selected as the option of the gradient item for spatial discretization. The pressure item is discretized by the Standard scheme. The second-order upwind scheme was utilized as spatial discretization method, while temperature discretization was implemented by first-order implicit time integration. The under-relaxation factors of density, pressure, momentum and energy are set to be 1.0, 0.15, 0.6 and 1.0, respectively. The definition of convergence criteria is based on the default Euclidean norm, and the absolute criteria for the continuity, momentum and energy equations are 10^{-3}, 10^{-3} and 10^{-6}, respectively. The maximum number of iterations allowed for each time step is set to 50. In addition, the simulation time for each operating condition is approximately 17 hours, and the specification of the computer used is shown in Table 1.

Table 1 Specification of the computer used

Computer	Specification
Name	DESKTOP - MRCTVBA
Operating system	Windows 10 Professional 64-bit
Processor	Intel(R) Xeon(R) Gold 6148 CPU @ 2.40GHz (40 CPUs), ~2.4GHz

The ice storage process of the smooth-tube heat exchanger and corrugated-tube heat exchanger in the present work were solved numerically. Firstly, the two-dimensional structural models of the two heat exchangers were established using SolidWorks and the whole domain was meshed by unstructured grid of quadrilateral meshes using ANSYS Meshing. The grid quality was checked to ensure the accuracy of numerical results. Then the mesh file was imported into ANSYS Fluent, where the gravity acceleration in y-direction was set to -9.81 m/s^2 and the type of time was set to Transient. Energy model, Laminar model and Solidification & Melting model were used as the calculation models, with the mushy zone constant ranging from 10^5 to 10^8. The simulation in this paper takes the commonly used value of 10^5 [43]. Moreover, fluid and solid materials were added according to the experimental materials and the User-Defined Functions (UDF) was coded to describe the variation of the density and thermal conductivity of water.

To ensure the accuracy of simulation results, the grid and time-step independence tests are conducted. Four different sizes of meshes of geometry with the number of

57729, 81843, 109475 and 146723 are analysed. The results of the liquid fraction are shown in Fig.5. It can be concluded that the predicted dynamic response of the liquid fraction for case with 109475 elements agrees well with that with 146723 elements. Moreover, the predicted liquid fraction for the case with time step of 0.1 s is same as the case with time step of 0.05 s. Therefore, based on accuracy and time cost, a grid number of 109475 and a time step of 0.1 s are selected in the present simulation model.

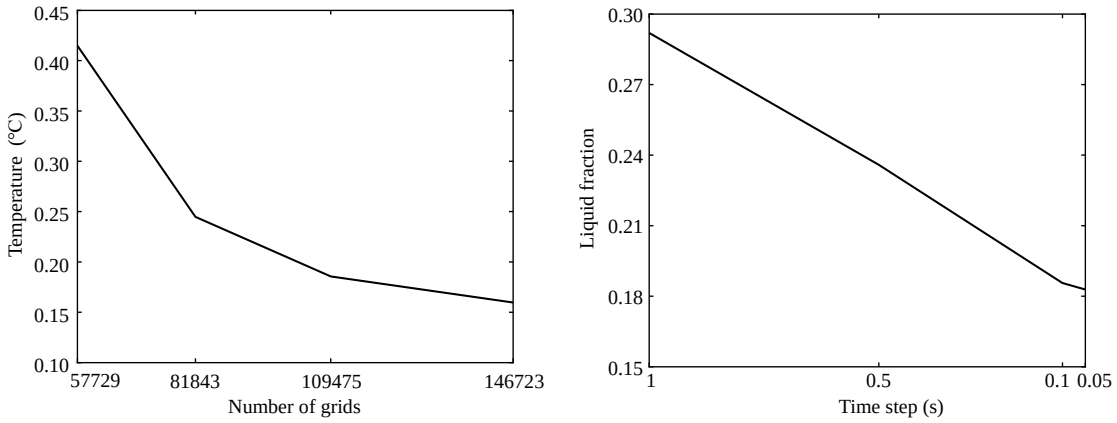

(a) Grid independence test (b) Time-step independence test

Fig. 5. Results of the independence tests

2.2 Experimental system

The experimental system is shown in Fig. 6 for the comparison experiment of smooth-tube and corrugated-tube heat exchangers. Fig. 7 shows the real experimental equipment. The experimental process and measurement equipments are same as those of our previous experiment in [44] and the experimental data used to verify the numerical model is adopted from the previous experiment. The model number and equipment parameters of experimental setup are listed in Table 2 and the uncertainty associated with each measurement value is summarized in Table 3.

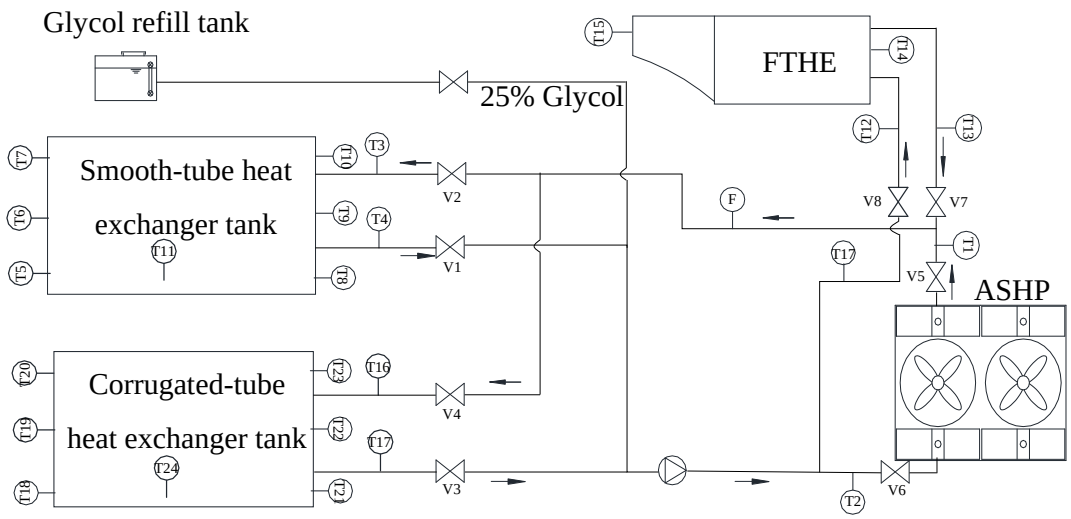

Fig. 6. Experimental system of ice storage

Fig. 7. Experimental system

Table 2 Introduction of experimental equipments

Equipment	air source heat pump chiller	finned tube heat exchanger
Model number	BK	ZK - 3.5D
Refrigerating capacity	28 kW	-
Rated air volume	-	3500 m^3/h
Rated voltage	380 V	380 V

Rated frequency	50 Hz	50 Hz
External residual pressure	-	210 Pa

Table 3 Accuracy of the measurement equipment

Equipment	Model	Range	Accuracy
Thermal resistances (temperature of the HTF)	PT100	-30 ℃ to 80 ℃	± 0.2 ℃
Flow meter (mass flow rate)	FS01A	2.3 - 23 m^3/h	± 0.0115 m^3/h
Datalogger: RTD input	GL840	-	± 0.6 ℃

3. Results and Discussion

3.1 Model validation

The boundary conditions of the numerical simulation are the same as those of experiment. The physical parameters of components of the ice-storage system are listed in Table 4.

Table 4 Physical parameters of components of the ice-storage system

physical parameters	water	ice	insulation （Outer wall）	stainless steel （tube wall）
Density (kg/m^3)	Eq. (9)	916	45	7930
Specific heat	4200	2100	1720	500

capacity [J/(kg·K)]				
Thermal conductivity [W/(m·K)]	0.55	2.22	0.02	16.3
Phase change temperature (℃)	0	0	-	-
Phase change heat (J/kg)	333146	333146	-	-
dynamic viscosity (kg/m·s)	0.001732	0.001732	-	-
Thermal expansion coefficient (1/K)	0.00013	-	-	-

The comparisons of the water temperature at center of the ice-storage tanks between simulation and experiment during the ice storage process are shown in Fig. 8. It can be seen that the curves of the experimental results and the simulation results are similar and consistent, and data errors are within 0.5 ℃. The root-mean-square error (RMSE) between the numerical and experimental results of the smooth-tube and corrugated-tube heat exchangers is 0.31 and 0.26 respectively, which meets the

accuracy requirements. During the phase change process, the system reaches a stable state and the simulated data meets the accuracy range of the temperature sensor used in the experiment.

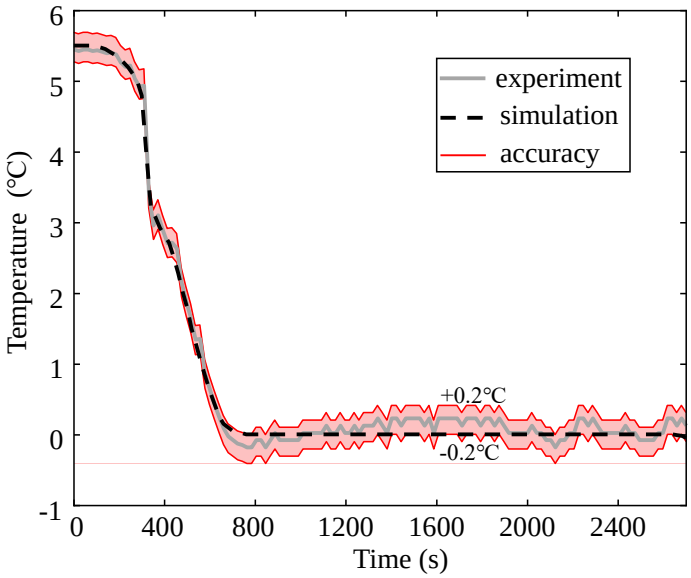

(a) Smooth-tube heat exchanger

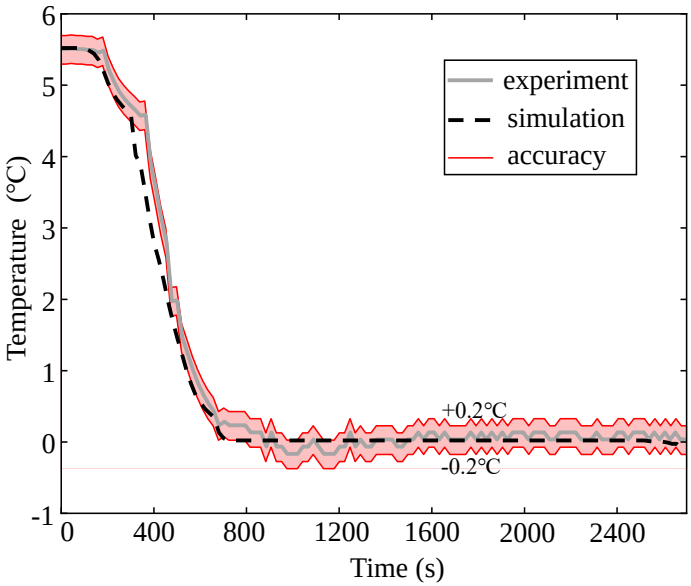

(b) Corrugated-tube heat exchanger

Fig. 8. Comparison of experiment and simulation between smooth-tube and corrugated-tube heat exchanger during the ice storage process

During the ice storage process in experiment, the water temperature at center of the ice-storage tanks is relatively stable at 0 ℃, and the status of PCM is mixture of ice and water. At around 2700 s, The simulation temperature of water decreases from the freezing temperature, while the experimental temperature remains at 0 ℃. This is because that during the experimental process, the status of PCM at center of the ice-storage tank is mixture of ice and water, which does not solidify completely. While the simulation simplifies the actual model to the two-dimensional model, where the PCM at the sampling point has already solidified with ice-storage time. The latent heat transfer between the PCM and the tube wall changes to the sensible heat transfer, resulting in the fact that the simulation of water temperature decreases after the phase change process.

3.2 Temperature and liquid fraction distribution

The temperature distribution variation with time at the radial section of the tubes during the ice storage process is shown in Fig. 9. After 150s of freezing, the temperature within the ice-storage tank has not reached the freezing point, and the status of PCM is liquid, which indicates that the heat transfer in the ice-storage tank is dominated by natural convection. During the early solidification process, the area of water is wide and the temperature of water in the upper part of the ice-storage tank is higher than those in the lower part due to natural convection. There is a rapid decrease of water temperature, while the variation of temperature becomes not obvious with the continuation of the ice storage process. This is because that the development of natural

convection during the ice storage process is negatively related to the thickness of ice. As the ice storage process continues, the thermal conduction of PCM gradually dominates such that the temperature variation of water accordingly slows down with the suppression of natural convection. The HTF absorbs the heat of water, and the water starts to solidify when the temperature reaches the freezing point. The ice formation is initially observed around the tube. The temperature distribution outside the radial section of the tubes is approximately circular and the temperature increases along the radial direction of the tubes.

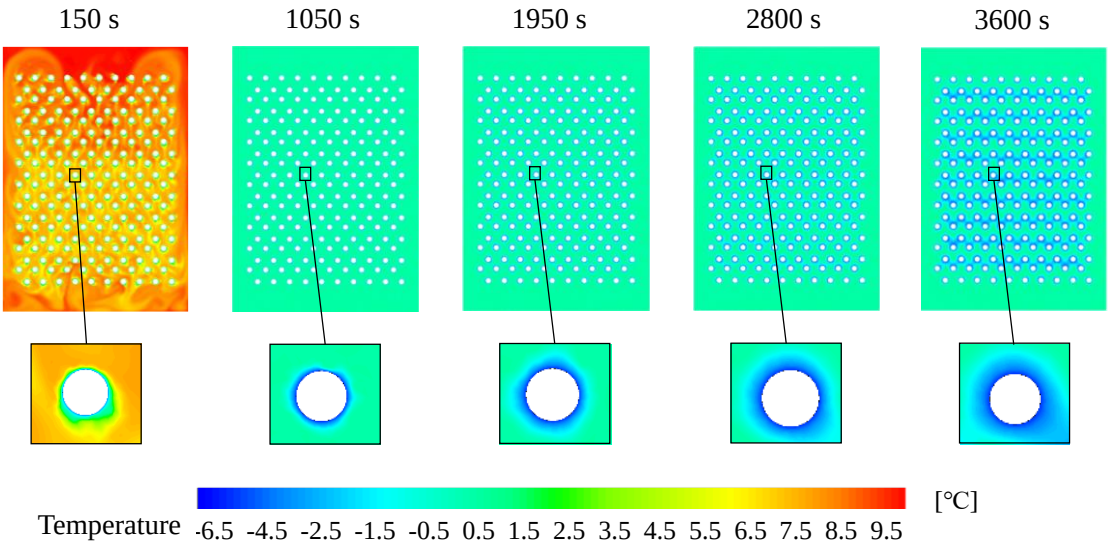

Fig. 9. Dynamic temperature distribution at the radial section of the tubes

Fig. 10 shows the liquid fraction distribution variation with time at the radial section of the tubes during the ice storage process. The ice formation is initially observed at the bottom round of the tubes. This is because of the natural convection. The water with lower density floats up and the water with higher density moves downward, resulting in more ice at the bottom round of the tubes in the initial stage of

the ice storage process. As the ice-storage time goes on, the shape of the ice becomes like a ring. As the ice layer develops, there is few difference of the ice formation between the upper and lower part of the tube. This is attributed to the suppression of natural convection caused by the thickness of the ice layer around the tubes. In addition, it can be observed that the degree of icing around tube at the top of the ice storage tank is much lower than that around the middle tube. This is because the freezing around the tube is affected by the surrounding temperature. Other tubes are distributed around the middle tube, with relatively low temperature, resulting in faster freezing rate. The upper tube, due to relatively high water temperature at the top of the tank, freezes slowly and the thickness of the ice layer shows a clear trend of thin up and thick down.

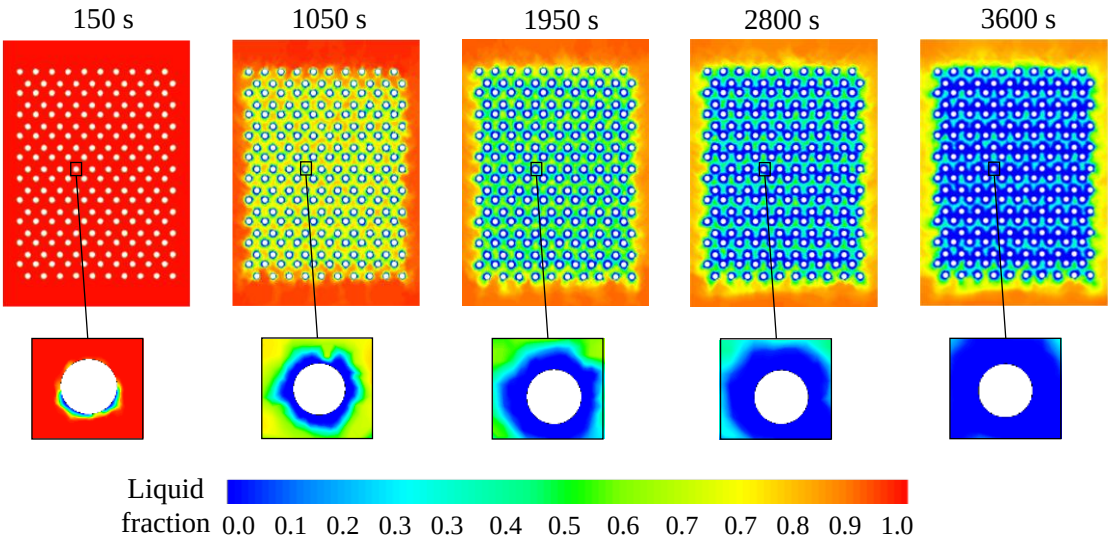

Fig. 10. Liquid fraction distribution at the radial section of the tubes

Having studied the formation of ice qualitatively, a quantitative analysis of liquid fraction versus time is carried out further. Figure 9 shows the inlet and outlet liquid fraction of PCM versus time of the smooth-tube and corrugated-tube heat exchangers.

When the liquid fraction declines from 1 to 0, it indicates that all the PCM around the tubes has accomplished the phase change process and turned out to be solid phase. As shown in Fig. 11, the liquid fraction distribution of the smooth-tube and corrugated-tube heat exchangers presents a similar downtrend. With the same cold storage capacity, the ice-storage simulated duration of the smooth-tube heat exchanger is 1980s, and the simulated duration of the corrugated-tube heat exchanger is 1840s, which is shortened by 7.1% compared with that of the traditional smooth-tube heat exchanger.

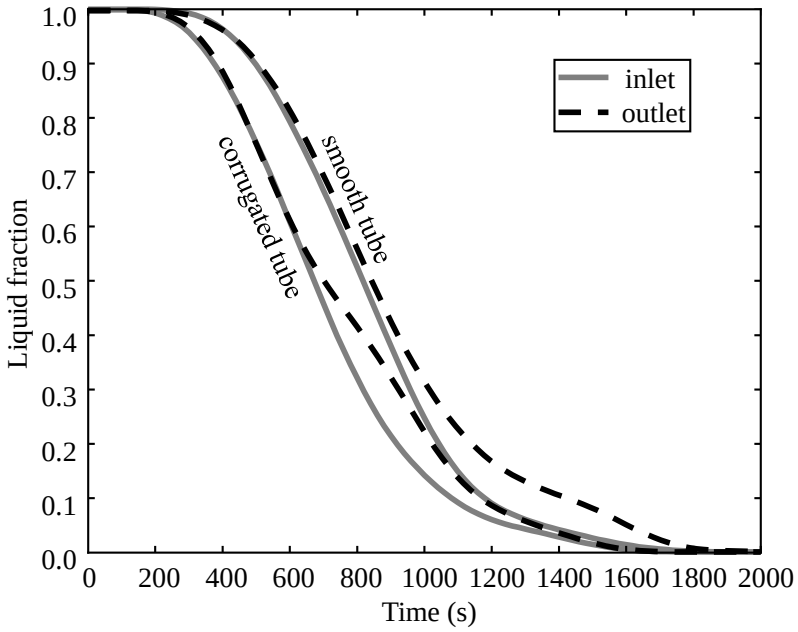

Fig. 11. Inlet and outlet liquid fraction versus time of the smooth-tube and corrugated-tube heat exchangers

By comparing the inlet and outlet liquid fraction, it can be indicated that the thickness of ice layer at different positions of the smooth-tube and corrugated-tube heat exchangers is different at the same time. The ice layer at the inlet of the tubes is thicker than that at the outlet of the tubes, since the low-temperature HTF entered the tube from

the inlet and the temperature difference between the PCM and the tube wall decreases gradually by heat transfer. The heat transfer from the PCM to the tube wall is reduced due to the increased accumulation of ice around the tubes, which is because of the increased thermal resistance of PCM. It is clear that the rate of ice accumulation at the outlet of the tubes decreases gradually with time, as the ice thickens. For the corrugated-tube heat exchanger, the change rate of the outlet liquid fraction is 2.58/h for the first 600s. It decreases to 2.22/h in the next 600s and becomes 0.56/h in the last 640s of the simulation. For the smooth-tube heat exchanger, the change rate of the outlet liquid fraction is 2.45/h for the first 1100s and decreases to 1.02/h in the last 880s.

Figure 12 shows the temperature distribution for the two heat exchangers in the initial stage of 500s. According to boundary layer theory [45], the fluid flow within the boundary layer is slow and the heat transfer is dominated by thermal conduction. Therefore, the temperature gradient in the near wall region is large. The corrugations disrupt the development of the boundary layer and strengthen the fluid mixing. Therefore, the heat transfer of corrugated-tube heat exchanger is enhanced compared with the smooth-tube heat exchanger.

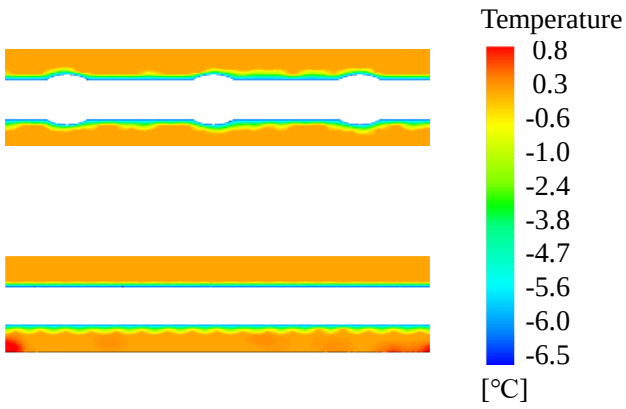

Fig. 12. Temperature distribution of the smooth-tube and corrugated-tube heat exchanger at 500s

Figure 13 depicts the liquid fraction distribution of smooth-tube and corrugated-tube heat exchangers during the ice storage process. At the same time, the ice outside the corrugated-tube heat exchanger is thicker than that outside the smooth-tube heat exchanger, which shows that the heat transfer effect of corrugated tube is superior than that of the smooth tube. This is because that the heat transfer area of corrugated tube is larger than that of the smooth tube and the corrugations change the fluid flow pattern outside the corrugated tube, which disrupt the development of the thermal boundary layer and improve the convective heat transfer performances.

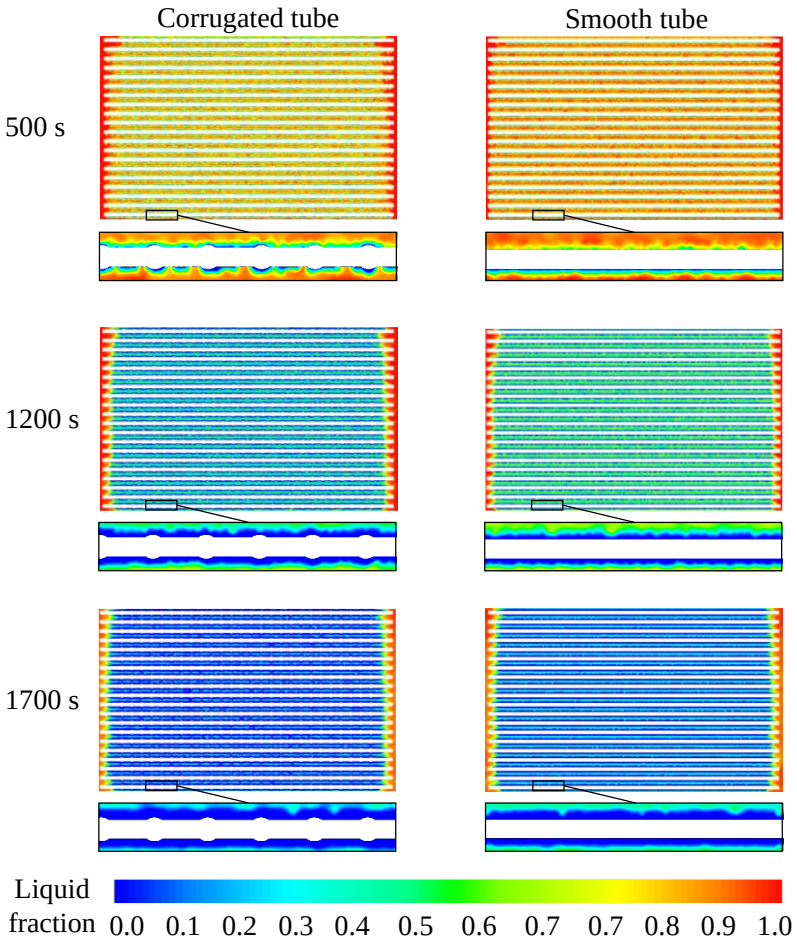

Fig. 13. Comparison of liquid distribution along the axial direction between the smooth-tube and corrugated-tube heat exchangers

3.3 Performance analysis of corrugation structural parameters

In this paper, the corrugation pitch and height are changed to study the effects of structural parameters of corrugated-tube heat exchanger on the ice storage performance. Considering that the corrugated tube structure with the pitch of 54mm and the height of 28mm is currently a commonly used size in engineering projects, and its processing is also relatively convenient. Therefore, the dimensions of other cases were fine-tuned based on this, which is less difficult for manufacturers to process and has low engineering processing cost.

3.3.1 Effect of corrugation pitch on ice storage performance

With the same cold storage capacity, corrugated tubes with corrugation pitch of 90mm (case 1), 54mm (case 2) and 37.5mm (case 3) are arranged in the ice storage tank. Figure 14 shows the liquid fraction distribution for three cases during the ice storage process. At the same time, the accumulation of ice outside the tubes increases with decreasing corrugation pitch, and the difference of ice thickness for the three cases becomes more and more obvious as the ice storage process continues. This is because that the heat transfer area between the PCM and the HTF is negatively related to the corrugation pitch. The heat exchanged increases with the increasing heat transfer area, resulting in the thicker ice layer outside the corrugated tubes with shorter corrugation pitch. While in the initial stage of ice storage process, the status of the PCM is liquid and the heat transfer is dominated by thermal convection. The turbulence of thermal

boundary layer is relatively strengthened within the corrugated-tube heat exchanger with short corrugation pitch, where the fixed ice layer is not easy to form. Therefore, there is no obvious difference of ice thickness for three cases at the initial stage of ice storage process. As the ice-storage time goes on, the ice layer thickens such that natural convection is suppressed and the thermal conduction of PCM gradually dominates. Therefore, the ice accumulation increases with the decreasing corrugation pitch.

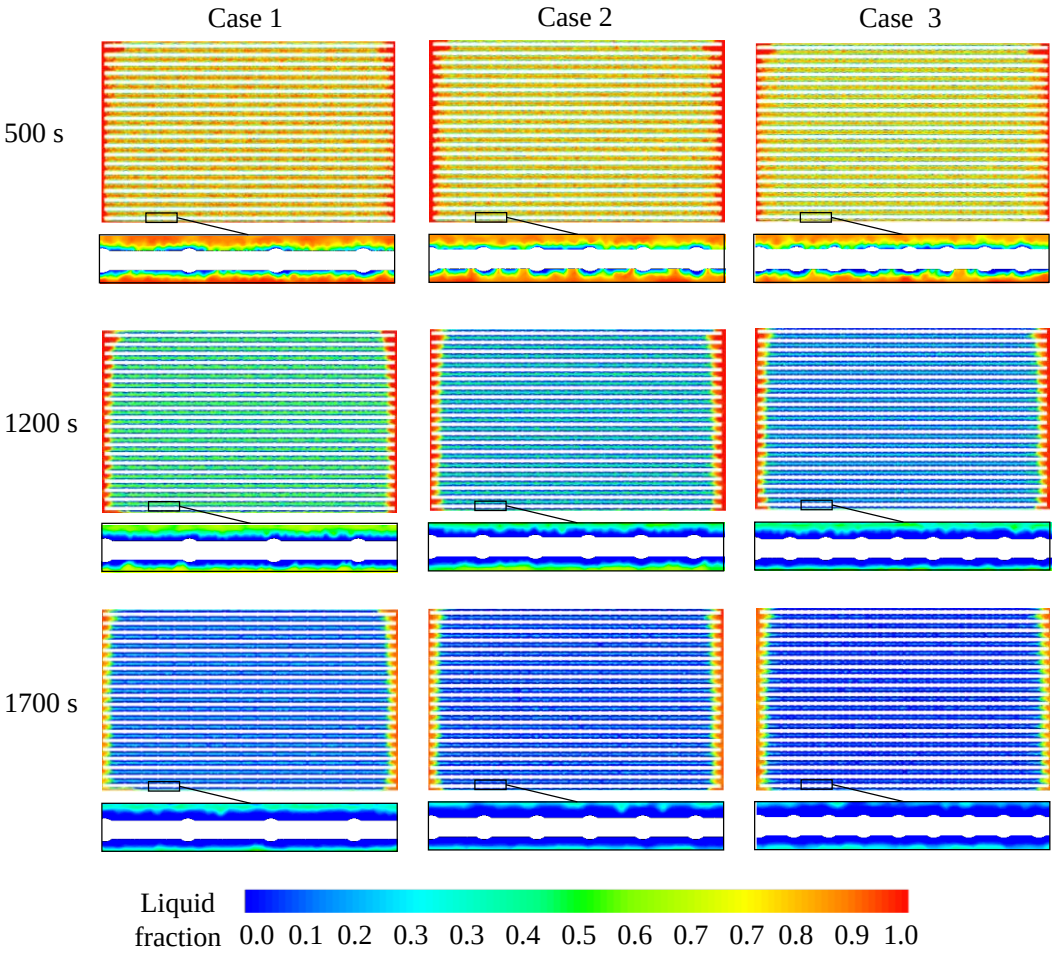

Fig. 14. Comparison of liquid fraction distribution along the axial direction for different corrugation pitch

To present a quantitative evaluation of the effect of corrugation pitch on the icing performance of the corrugated-tube heat exchanger, Fig. 15 depicts the liquid fraction

near the wall of the tube outlet for three cases. It is seen that the ice storage duration of the case with shorter corrugation pitch is shorter. The ice storage duration of case 2 and case 3 is 1840s and 1740s respectively, which is shortened by 5.2% and 10.3% compared with that of case 1.

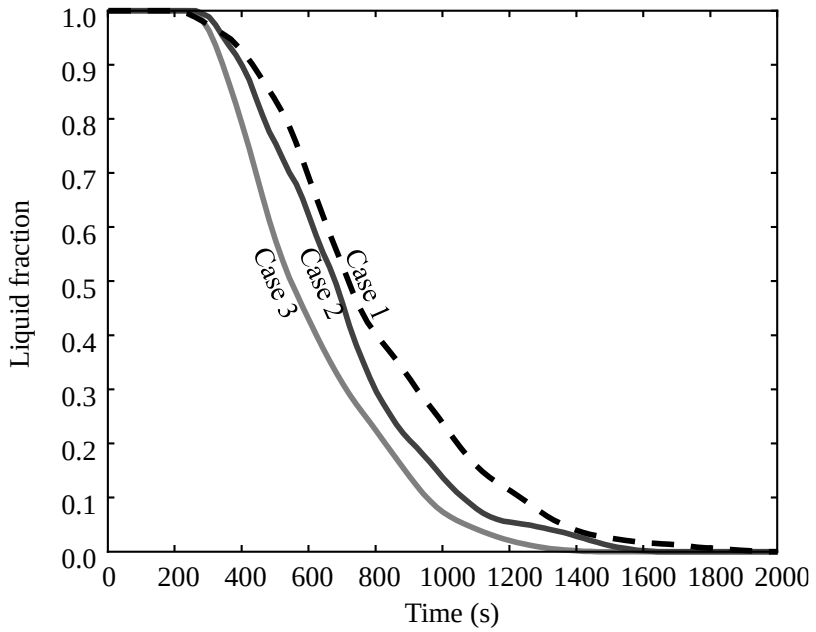

Fig. 15. Comparison of liquid fraction distribution versus time at the tube outlet for different corrugation pitch

3.3.2 Effect of corrugation height on ice storage performance

With the same cold storage capacity, corrugated tubes with corrugation height of 25mm (case 2), 28mm (case 4) and 32mm (case 5) are arranged in the ice storage tank. Figure 16 shows the liquid fraction distribution for three cases during the ice storage process. In the initial stage of 500s, there is no significant difference of ice formation for three cases. As the ice storage process continues, the corrugated tube heat exchanger has been covered with ice at the time of 900s, and the thickness of ice increases with

the increasing corrugation height. This is because that the heat transfer area between the PCM and the HTF is positively related to the corrugation height. While in the initial stage of ice storage process, the heat transfer is dominated by thermal convection. The turbulence of thermal boundary layer is relatively strengthened within the corrugated-tube heat exchanger with high corrugation height, where the fixed ice layer is not easy to form. Therefore, there is no obvious difference of ice thickness for three cases in the initial stage of ice storage process. As the ice-storage time goes on, the ice layer thickens such that natural convection is suppressed and the thermal conduction of PCM gradually dominates. Therefore, the ice accumulation increases with the increasing corrugation height.

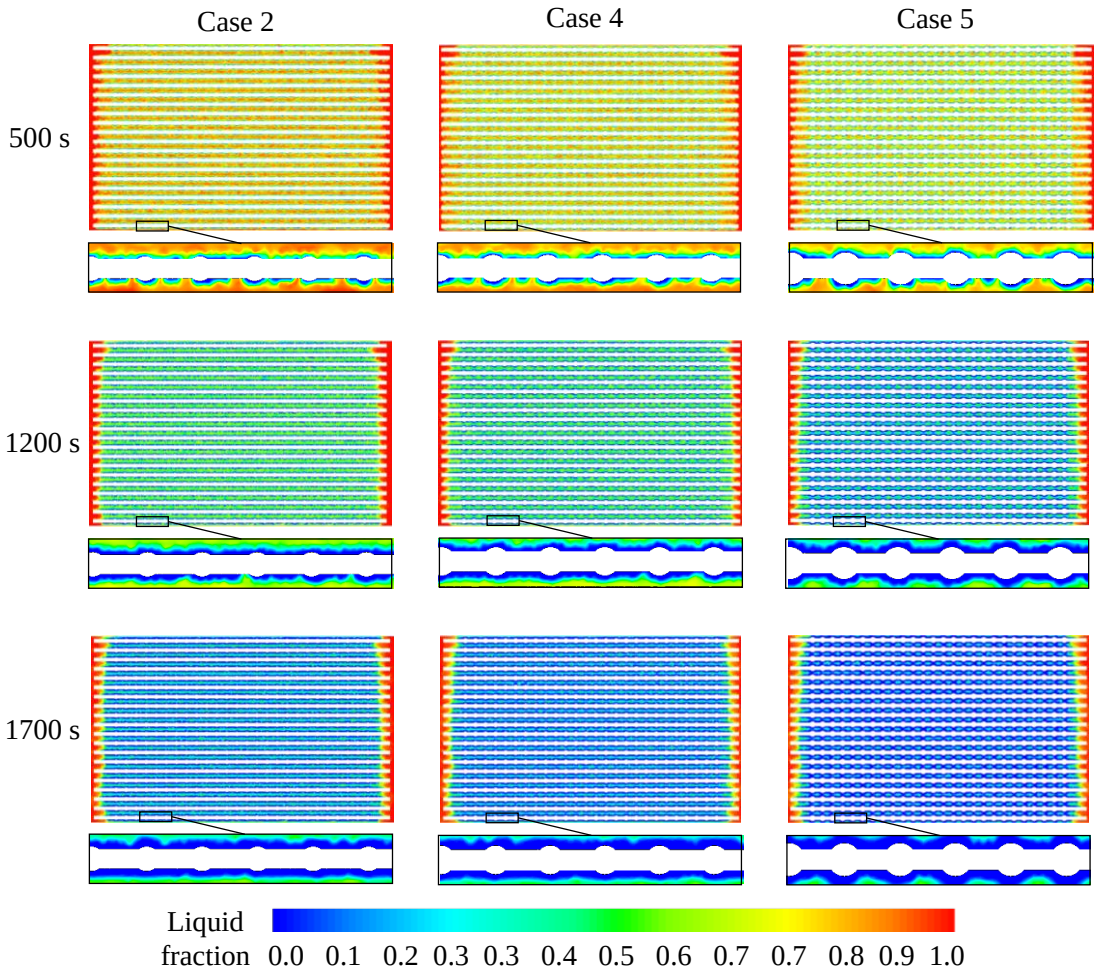

Fig. 16. Comparison of liquid fraction distribution along the axial direction for different corrugation heights

Fig. 17 depicts the liquid fraction near the wall of the tube outlet for three cases. It is seen that the ice storage duration of the case with higher corrugation height is shorter. The ice storage duration of case 4 and case 5 is 1680s and 1300s respectively, which is shortened by 8.7% and 29.4% compared with that of case 2.

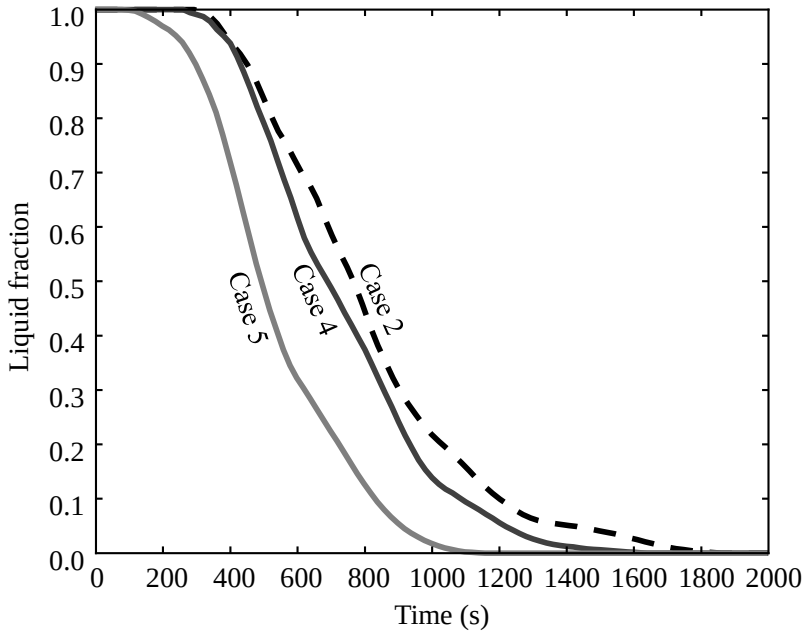

Fig. 17. Comparison of liquid fraction distribution versus time at the tube outlet for different corrugation pitch

The results show that with the same cold storage capacity, the heat transfer effect of corrugated-tube heat exchanger increases with the decreasing corrugation pitch and the increasing corrugation height. Compared with the effect of corrugation pitch on heat transfer performance of corrugated-tube heat exchanger, the effect of corrugation height

is more significant.

4. Conclusions

In this study, the two-dimensional models solved by Computational fluid dynamics (CFD) are used to simplify and analyze the ice storage system for smooth-tube heat exchanger and corrugated-tube heat exchanger. The temperature and liquid fraction distribution characteristics are studied to analyze the heat transfer enhancement mechanisms of the corrugated-tube heat exchanger. In addition, the effects of corrugation structural parameters on the heat transfer performances of the corrugated-tube heat exchanger are investigated. In our future work, we will further study and analyze the flow characteristics of fluid in symmetrical outward corrugated tube heat exchangers. The conclusions of this study are drawn as follow:

(1) The simulation results are basically consistent with the experimental results. The root-mean-square error between the numerical and experimental results of smooth-tube and corrugated-tube heat exchanger is 0.31 and 0.26, respectively, which proves that the numerical model is feasible for ice storage performance prediction. It is reasonable and reliable to investigate ice storage performances based on the prediction of the model.

(2) During the early solidification process, the ice formation is initially observed at the bottom round of the tubes. As the ice-storage time goes on, the shape of the ice becomes like a ring and the heat transfer is dominated by thermal conduction instead of natural convection.

(3) The thickness of ice layer at corresponding position of the two heat exchangers is different at the same time. The ice thickness gradually decreases along the axial direction of the tubes, and the rate of ice accumulation at outlet of the tubes decreases gradually with time. For the corrugated-tube heat exchanger, the change rate of the outlet liquid fraction decreases by 78.3%. For the smooth-tube heat exchanger, the change rate of the outlet liquid fraction decreases by 58.4%.

(4) The corrugation disrupts the boundary layer development, strengthens the turbulence mixing and reduces the temperature gradient in the boundary layer, thus enhancing the heat transfer. Under the same conditions, the ice-storage duration of the corrugated-tube heat exchanger is shortened by 7.1% compared with that of the smooth-tube heat exchanger.

(5) The ice storage performance enhances with the decreasing corrugation pitch and the increasing corrugation height. If the corrugation pitch decreases by 40% and 58.3%, the ice storage duration of corrugated-tube heat exchanger is shortened by 5.2% and 10.3%, respectively. If the corrugation height increases by 12% and 28%, the ice storage duration of corrugated-tube heat exchanger is shortened by 8.7% and 29.4%, respectively.

Acknowledgement

This work was supported by the National Natural Science Foundation of China (No. 52008290).

References

[1] C. John, H. Paul, D. Jim, L. Angelina, T. James T., W. Lynn. International Energy Outlook 2016 with projections to 2040. USDOE Energy Information Administration (EIA), Washington, DC (United States), 2016.

[2] H.H. Sait, Design and analysis of a flooded tube for cold energy storage. International Journal of Refrigeration, 94 (2018) 151-160.

[3] Y. Tian, M. Zheng, D. Fan, Y. Zhang, J. Zhao, G. Jin, W. Wu, E. Cuce, S. Gou. A novel latent heat storage unit by introducing jet breakup of phase change material. Journal of Energy Storage, 49 (2022) 104070.

[4] A. López-Navarro, J. Biosca-Taronger, B. Torregrosa-Jaime, J.M. Corberán, J.L. Bote-Garcia, J. Payá. Experimental investigations on the influence of ice floating in an internal melt ice-on-coil tank. Energy and Buildings, 57 (2013) 20-25.

[5] F.L. Tan, S.F. Hosseinizadeh, J.M. Khodadadi, L. Fan. Experimental and computational study of constrained melting of phase change materials (PCM) inside a spherical capsule. International Journal of Heat and Mass Transfer, 52 (15-16) (2009) 3464-3472.

[6] T. Asaoka, Y. Endo. Experimental study on absorption ice slurry generator with ethanol solution as the refrigerant. International Journal of Heat and Mass Transfer, 162 (2020) 120333.

[7] M.A. Ezan, M. Ozdogan, A. Erek. Experimental study on charging and discharging periods of water in a latent heat storage unit. International Journal of Thermal Sciences, 50 (11) (2011) 2205-2219.

[8] A. Fertelli. Air-conditioning system with ice thermal storage. Cukurova Universitesi Fen Bilimleri Enstitusu, 2008. http://libratez.cu.edu.tr/tezler/6817.

[9] Y. Bi, M. Yu, H. Wang, J. Huang, T. Lyu. Experimental investigation of ice melting system with open and closed ice-storage tanks combined internal and external ice melting processes. Energy and Buildings, 194 (2019) 12-20.

[10] Y. Cao, Y. Jiang, B. Song, S. Jiang, L. Yu. Numerical Simulation and Experiment Study on Dynamic Freezing Characteristics of Ice-on-Coil. Journal of Nanjing University of Aeronautics & Astronautics, 39(6) (2007) 756-760 [In Chinese].

[11] H. Zhou, M. Chen, X. Han, P. Cao, F. Yao, L. Wu. Enhancement Study of Ice Storage Performance in Circular Tank with Finned Tube. Processes, 7(5) (2019) 266. https://doi.org/10.3390/pr7050266.

[12] A.M. Fsadni, J.P.M. Whitty. A review on the two-phase pressure drop characteristics in helically coiled tubes. Applied Thermal Engineering, 103 (2016) 616-638.

[13] Y. Li, C. Yang, Z. Yan, B. Gou, H. Yuan, J. Zhao, N. Mei. Analysis of the icing and melting process in a coil heat exchanger. Energy Procedia, 136 (2017) 450-455.

[14] N. Ghorbani, H. Taherian, M. Gorji, H. Mirgolbabaei. Experimental study of mixed convection heat transfer in vertical helically coiled tube heat exchangers. Experimental Thermal and Fluid Science, 34(7) (2010) 900-905.

[15] F. Afsharpanah, K. Pakzad, S.S.M. Ajarostaghi, S. Poncet, K. Sedighi. Accelerating the charging process in a shell and dual coil ice storage unit equipped with connecting plates. Energy Research, 46(6) (2022) 7460-7478.

[16] T. Yang, Q. Sun, R. Wennersten. The impact of refrigerant inlet temperature on the ice storage process in an ice-on-coil storage plate. Energy Procedia, 145 (2018) 82-87.

[17] F. Afsharpanah, K. Pakzad, S.S.M. Ajarostaghi, M. Arici. Assessment of the charging

performance in a cold thermal energy storage container with two rows of serpentine tubes and extended surfaces. Journal of Energy Storage, 51 (2022) 104464.

[18] J. Du, R. Wang, Q. Zhuo, W. Yuan. Heat transfer enhancement of Fe_3O_4-water nanofluid by the thermo-magnetic convection and thermophorestic effect. Int. J. Energy Res., 46(7) (2022) 9521-9532.

[19] F. Afsharpanah, M. Izadi, F.A. Hamedani, S.S.M. Ajarostaghi, W. Yaici. Solidification of nano-enhanced PCM-porous composites in a cylindrical cold thermal energy storage enclosure. Case Studies in Thermal Engineering, 39 (2022) 102421.

[20] M. Zaboil, S. Saedodin, S.S.M. Ajarostaghi, M. Nourbakhsh. Numerical evaluation of the heat transfer in a shell and corrugated coil tube heat exchanger with three various water-based nanofluids. Heat Transfer, 50(6) (2021) 6043-6067.

[21] F. Afsharpanah, S.S.M. Ajarostaghi, F.A. Hamedani, M.S. Pour. Compound Heat Transfer Augmentation of a Shell-and-Coil Ice Storage Unit with Metal-Oxide Nano Additives and Connecting Plates. Nanomaterials, 12(6) (2022) 1010.

[22] A. Laouer, M. Arici, M. Teggar, S. Bouabdallah, C. Yilidiz, K.A.R. Ismail, S.S.M. Ajarostaghi, E.H. Mezaache. Effect of Magnetic Field and Nanoparticle Concentration on Melting of Cu-Ice in a Rectangular Cavity under Fluctuating Temperatures. Journal of Energy Storage, 36 (2021) 102421.

[23] Y.Zhang, A. Faghri. Heat transfer enhancement in latent heat thermal energy storage system by using the internally finned tube. International Journal of Heat and Mass Transfer, 39(15) (1996) 3165-3173.

[24] Q. Hu, X. Qu, W. Pen, J. Wang. Experimental and numerical investigation of turbulent heat transfer enhancement of an intermediate heat exchanger using corrugated tubes. International

Journal of Heat and Mass Transfer, 185 (2022) Article 122385.

[25] H. Jannesari, N. Abdollahi. Experimental and numerical study of thin ring and annular fin effects on improving the ice formation in ice-on-coil thermal storage systems. Applied Energy, 189 (2017) 369-384.

[26] F. Agyenim, P. Eames, M. Smyth. A comparison of heat transfer enhancement in a medium temperature thermal energy storage heat exchanger using fins. Solar Energy, 83(9) (2009) 1509-1520.

[27] K.A.R. Ismail, F.A.M. Lino. Fins and turbulence promoters for heat transfer enhancement in latent heat storage systems. Experimental Thermal and Fluid Science, 35(6) (2011) 1010-1018.

[28] F. Agyenim, S.S.M. Ajarostaghi, M. Arici. Parametric study of phase change time reduction in a shell-and-tube ice storage system with anchor-type fin design. International Communication in Heat and Mass Transfer, 137 (2022) 106281.

[29] D. Yang, H. Li, T. Chen. Pressure drop, heat transfer and performance of single-phase turbulent flow in spirally corrugated tubes. Experimental Thermal and Fluid Science, 24 (2001) 131-138.

[30] H. Olfian, S.S.M. Ajarostaghi, M. Farhadi, A. Ramiar. Melting and solidification processes of phase change material in evacuated tube solar collector with U-shaped spirally corrugated tube. Applied Thermal Engineering 182 (2021) 116149.

[31] M. Zaboli, M. Nourbakhsh, S.S.M. Ajarostaghi. Numerical evaluation of the heat transfer and fluid flow in a corrugated coil tube with lobe-shaped cross-section and two types of spiral twisted tape as swirl generator. Journal of Thermal Analysis and Calorimetry, 147 (2022) 999-1015.

[32] X. Li, J. Meng, Z. Li. Roughness enhanced mechanism for turbulent convective heat transfer. International Journal of Heat and Mass Transfer, 54(9-10) (2011) 1775-1781.

[33] H.K. Moghadam, S.S.M. Ajarostaghi, S. Poncet. Extensive numerical analysis of the thermal performance of a corrugated tube with coiled wire. Journal of Thermal Analysis and Calorimetry, 140 (2020) 1469-1481.

[34] Ö. Ağra, H. Demir, S.Ö. Atayilmaz, F. Kantas, A.S. Dalkilic. Numerical investigation of heat transfer and pressure drop in enhanced tubes. International Communications in Heat and Mass Transfer, 38(10) (2011) 1384-1391.

[35] J. Hærvig, K. Sørensen, T.J. Condra. On the fully-developed heat transfer enhancing flow field in sinusoidally, spirally corrugated tubes using computational fluid dynamics. International Journal of Heat and Mass Transfer, 106 (2017) 1051-1062.

[36].H.A. Mohammed, A.K. Abbas, J.M. Sheriff. Influence of geometrical parameters and forced convective heat transfer in transversely corrugated circular tubes. International Communications in Heat and Mass Transfer, 44 (2013) 116-126.

[37] F. Afsharpanah, G. Cheraghian, F.A. Hamedani, E. Shokri, S.S.M. Ajarostaghi. Utilization of Carbon-Based Nanomaterials and Plate-Fin Networks in a Cold PCM Container with Application in Air Conditioning of Buildings. Nanomaterials, 12(11) (2022) 1927.

[38] V.R. Voller, A.D. Brent, C. Prakash. The modelling of heat, mass and solute transport in solidification systems. International Journal of Heat and Mass Transfer, 32 (9) (1989) 1719-1731.

[39] Y. Tian, C. Chen, T. Lu, H. Yang, Y. Luo, X. Cheng. Numerical simulation of the heat storage performance of heat storage tanks containing phase change materials. Journal of Beijing University of Chemical Technology (Natural Science), 49 (4) (2022) 83-90 [In Chinese].

[40] K.Yang, N.Zhu, C. Chang, H. Yu, S. Yang. Numerical analysis of phase-change material melting in triplex tube heat exchanger. Renewable Energy, 145 (2020) 867-877.

[41] X. Jia, X. Zhai, X. Cheng. Thermal performance analysis and optimization of a spherical PCM capsule with pin-fins for cold storage. Applied Thermal Engineering, 148 (2019) 929-938.

[42] R.M. Fand, B.Y.K. Kim, A.C.C. Lam, R. T. Phan. Resistance to the flow of fluids through simple and complex porous media whose matrices are composed of randomly packed spheres. Journal of Fluids Engineering, 109 (3) (1987) 268-273.

[43] A.C. Kheirabadi, D. Groulx. The effect of the mushy-zone constant on simulated phase change heat transfer, Proceedings of CHT-15 ICHMT International Symposium on Advances in Computational Heat Transfer, 25 May - 29 May, Rutgers University, Piscataway, USA. (2015).

[44] C. Li, J. Hou, Y. Wang, S. Wei, P. Zhou, Z. He, Y. Wang, H. Zhang, S. You. Dynamic heat transfer characteristics of ice storage in smooth-tube and corrugated-tube heat exchangers. Applied Thermal Engineering, 223 (2023) 120037.

[45] H. Schlichting, K. Gersten. Boundary-Layer Theory, Springer, 2017. https://citations.springernature.com/book?doi=10.1007/978-3-662-52919-5.